Towards next-generation SPR-based biosensors with machine learning technologies

1st Nkgaphe Tsebesebe
National Laser Centre
Council for Scientific and Industrial Research
Pretoria, South Africa
ntsebesebe@csir.co.za

2nd Kelvin Mpofu
National Laser Centre
Council for Scientific and Industrial Research
Pretoria, South Africa
KMpofu@csir.co.za

3rd Sudesh Sivarasu
Division of Biomedical Engineering
University of Cape Town
Western Cape, South Africa
Sudesh.Sivarasu@uct.ac.za

4th Patience Mthunzi-Kufa
School of Interdisciplinary Research and Graduate Studies (UNESCO)
University of South Africa
Pretoria, South Africa
patiencemthunzi@gmail.com

***Abstract*— In clinical investigation of biomolecular interactions, surface plasmon resonance imaging (SPRi), a label-free detection technique, has proven to be an appropriate and dependable platform. A useful option for biosensing platforms is surface plasmon resonance-based sensors because of their excellent sensitivity and fine resolution. However, the detection limit of the SPRi-based detection method is limited by its relatively poor signal-to-noise ratio. Machine learning (ML) approaches therefore have the potential to address these problems. Machine learning techniques can help create SPR sensors more efficiently and increase their performance by automating the diagnostic process and increasing the signal-to-noise ratio. In this work, SPRi images are used to train the k-nearest neighbor algorithm for image classification. The KNN model correctly predicted all SPRi images in the dataset by achieving 100% accuracy, sensitivity, and specificity. With an AUC of 1.0, the model performed excellently, suggesting exceptional potential for automated real-time detection of binding events. Therefore, the machine learning-enhanced SPRi platform has the potential to offer a robust alternative to conventional manual interpretation in SPR sensing.**

Keywords*— *surface plasmon resonance imaging, machine learning, classification binding, nonbinding

I. Introduction

Surface Plasmon Resonance Imaging (SPRi) is an optical sensing technique widely utilized for real-time, label-free monitoring of biomolecular interactions at sensor surfaces [1]. Surface Plasmon Resonance Imaging builds upon the fundamental principle of Surface Plasmon Resonance (SPR), where incident light induces collective oscillations of free electrons at the metal-dielectric interface, resulting in an evanescent field highly sensitive to refractive index changes near the surface [1,2]. This sensitivity makes SPRi highly valuable for detecting binding events in complex biological samples, with applications in drug discovery, disease diagnostics, and environmental monitoring.

Despite its promise, SPRi suffers from intrinsic limitations such as low signal-to-noise ratios, difficulty in resolving weak binding events, and significant reliance on manual image interpretation. These challenges can result in lower sensitivity and hinder the broader adoption of SPRi in clinical diagnostics. Recent advances in artificial intelligence, particularly machine learning (ML), offer a compelling solution to these problems [3]. ML algorithms are capable of extracting subtle patterns from high-dimensional data, automating image classification, and enhancing analytical performance in noisy environments.

In biosensing contexts, ML has been successfully applied to improve the specificity and sensitivity of optical sensors by reducing background noise, classifying spectral responses, and enhancing feature selection and data interpretation. For instance, convolutional neural networks (CNNs), support vector machines (SVMs), and K-nearest neighbours (KNN) have been used to detect analyte-binding events and improve diagnostic accuracy across different sensor modalities, including electrochemical and SPR-based platforms [2,3]. Studies such as Huo *et. al.* and Kaziz *et. al*. have emphasized the role of ML in optimizing biosensor outputs by increasing signal fidelity and reducing the burden on manual interpretation [4,5].

In this study, we propose the integration of a k-nearest neighbour machine learning classifier with SPRi image datasets to address the signal interpretation and classification challenges. By taking a dataset of SPRi images (**Fig. 1**) and training the classifier to distinguish between binding and non-binding conditions, we aim to establish a robust and reproducible framework that enhances the sensitivity and reliability of SPRi detection platforms. The integration of artificial intelligence and biosensing represents a technological evolution in the healthcare space. This work contributes to the growing body of evidence supporting the hybridization of machine learning with label-free biosensing for rapid, accurate, and automated diagnostics.

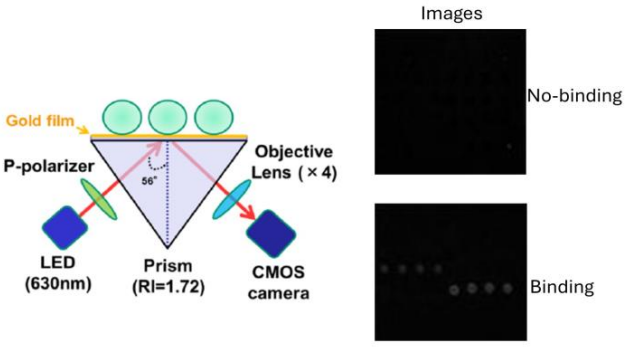

Fig. 1. A principle of surface plasmon resonance.

II. METHODOLOGY

A. Input Data and Preprocessing

This study considered a supervised machine learning approach to perform binary classification. The KNN algorithm was trained on labelled images to predict outcomes and outputs a categorical label that represents either the binding or nonbinding class. The non-binding and binding classes are represented numerically with 0 and 1, respectively. These classes contained images from the SPR experiment where the binding images resemble white dots on the images as shown in **Fig.1**. On the other hand, the non-binding images does not have the dots, they are only black images. The dots on the images are used to distinguish the images into their respective classes. The images used in this study were obtained from a publicly website for scientific and analytical instruments [14].

A balanced dataset of 200 images was used in each class to ensure that the model does not bias towards classes during training. The dataset was split into an 8:2 ratio, where 320 images (160 for binding and 160 for nonbinding) were used to train the KNN algorithm, and 80 images (40 for binding and 40 for non-binding) were used to test the performance of the KNN model. Before training and testing, all images in the classes were resized to 224 x 224 pixels, followed by transforming their 2-dimensional array representation into a single-dimensional array of 50,176 elements, each containing a pixel value. The pixel values were scaled to a common range of 0 and 1 to help improve the performance of the model. This was achieved by dividing the pixel values in the array by the maximum value of an 8-bit image (255). The binary values, 0 and 1, represent black and white colours, respectively, to provide the intensity information of the light. Lastly, the KNN algorithm was trained and validated on the new images. This work used default parameter for a KNN in scikit-learn as: neighbours=5, weights='uniform', algorithm='auto', leaf_size=30, p=2, and metric='minkowski'. In **Fig. 2** is the summarized process of training the machine learning algorithm of this study.

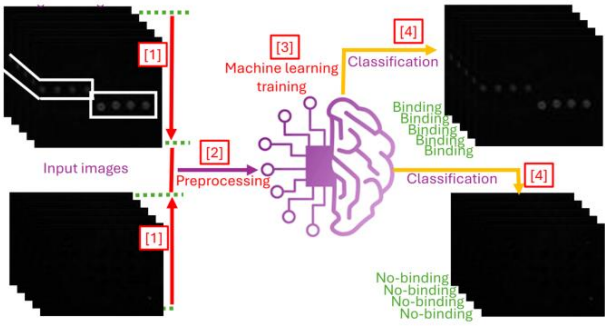

Fig. 2 The methodology of training the KNN model in this study.

B. K-nearest neighbor machine learning classifier

The K-Nearest Neighbours (KNN) algorithm is a nonparametric supervised learning technique used for both classification and regression tasks to find the nearest data points to a new data point and make predictions based on the majority class or the average value of the neighbours [6,7]. In this work, white spots, which represent binding, are used as features to calculate the distance between the data points. The data of each image was represented as a feature vector:

$$x = [\, x_1, x_2, \ldots, x_n] \tag{1}$$

Where x is a feature vector, x_i is an individual feature, and n is the total number of features. The distance from the two points x_i and x_j in the dataset is computed from the Euclidean distance formula [6,8]:

$$d(x_i, x_j) = \sqrt{\sum_{k=1}^{n} (x_{ik} - x_{jk})^2} \tag{2}$$

where $d(x_i, x_j)$ represents a distance between the two points, and n represents the total number of features. For every new data point x_{new}, distances of all points in the data set are calculated, and the smallest distance k is the k nearest neighbour [6]. Then the predicted class y_{new} of x_{new}, is determined from a majority vote among the nearest neighbours as follows:

$$y_{new} = mode\,\{y_{i1}, y_{i2}, \ldots, y_{ik}\} \tag{3}$$

Where y_{ij} is the class of the j^{th} nearest neighbor to x_{new}. In the context of this work y_{new} can be 1 to represent binding and 0 to represent nonbinding.

C. K-nearest neighbor machine learning classifier

In this study, quantitative indicators such as accuracy, sensitivity, specificity, precision, and F1-score were used to evaluate the prediction performance of the KNN. The focus was on four output parameters, as explained below:

- **True Positive (TP)**: The number of images with binding spots that are predicted to be binding.
- **True Negative (TN)**: The number of images with no spots that are predicted as nonbinding
- **False Positive (FP)**: The number of images with no spots that are predicted to be binding.
- **False Negative (FN)**: The number of images with binding spots that are predicted to be nonbinding.

The parameters were used to determine the qualitative indicators described as follows.

- **Accuracy**: The accuracy measure was used to determine the classification performance of the KNN by evaluating its ability to correctly predict all images in the data set. The accuracy measure was determined as [9-12]:

$$Accuracy = \frac{TP + TN}{TP + TN + FP + FN} * 100 \tag{4}$$

- **Sensitivity**: The sensitivity measure was used to determine how accurately the KNN model distinguished the image features. The sensitivity percentage was calculated as [9-12]:

$$Sensitivity = \frac{TP}{FN + TN} * 100 \tag{5}$$

- **Precision**: The precision measure was used to analyse the images predicted as binding by evaluating the relationship ratio between the correctly predicted binding images and all predicted images. The calculations were performed from [9-12]:

$$Precision = \frac{TP}{TP + FP} * 100 \quad (6)$$

- **Specificity**: The specificity measure was used to identify a number of true negatives that were correctly predicted in the image dataset. This represented the ability of the KNN to correctly predict nonbinding images from all the images in the input dataset. The percentage of specificity was determined as [9-12]:

$$Specificity = \frac{TP}{TP + FP} * 100 \quad (7)$$

- **F1-score**: The F1-score was used to assess the balance between precision and sensitivity/recall as follows [9-12]:

$$F1 - score = \frac{2 \times TP}{2 * TP + FN + FP} * 100 \quad (8)$$

III. Model Performance

The KNN classification performance was evaluated from a confusion matrix shown in **Fig. 3**. The models correctly predicted all 40 images with binding spots into the binding class and all 40 images without binding spots into the nonbinding class. As such, the model recorded 0% false positives and false negatives. The clinical indicator in **Table 1** further illustrates that the KNN model was able to correctly predict all images in the dataset by achieving 100% accuracy. This was also noted in the 100% sensitivity, which suggested that the model was able to distinguish the image features, leading to a higher ratio between correctly predicted binding images and all predicted images. This provides more evidence that the model was also able to correctly predict non-binding images from all the images in the input dataset. The F1-score of 100% also supported perfect precision and recall by indicating that the model correctly predicted all images across the entire dataset. The generalizability of the model on the new dataset proved to be excellent, as the training and testing scores were equal (**Table 2**), indicating that there was no overfitting. This was further validated by an area under a receiver operating characteristic curve (**Fig. 4**), which indicated an excellent binary classification by recording 1.0. The performance of the model was further compared with other machine learning models for binary classifications as shown in **Table 1.**

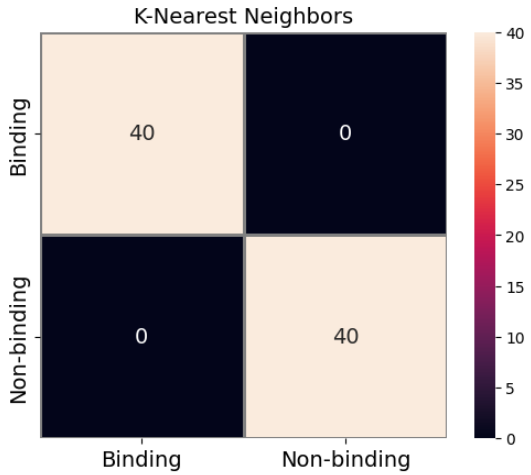

Fig. 3 A representation of a confusion matrix for evaluating the classification performance of the KNN.

For this specific binding and nonbinding prediction task, it is evident that the KNN-based model achieved a notably higher accuracy. This can be associated with simplicity in the data set, which only had two features, resulting in a higher quality of images that can be linearly separable. Manual balancing of the images in both classes ensured that the model was not biased toward the images during training, leading to high performance. The performance was further improved and made stable by normalized features with a comparable scale. Although the performance of the KNN in this study is exceptionally high, increasing the data set could increase computational cost since the model is instance-based [6]. Model performance could further be degraded with high-dimensional data [6]. As such, this study focused on exploring the strengths of KNN to extend its applications in SPRi. Since the KNN is nonparametric, it does not make assumptions about the data distribution, which has potential for automated detection of binding events.

The KNN model in general can be implemented and it is adaptable, which allows it to be updatable in the presence of new data [6]. However, the model suffers from several limitations such as, computational intensity, feature dependence and dimensionality [6]. That is large dataset can be computationally expensive when considering the KNN due to its instance-base structure. Furthermore, the performance of the model is subjected to degradation with high-dimensional data. Another major factor that has a potential to directly affect the performance of the model are the features used, from where the inessential feature can have a negative effect on the accuracy of the model [6].

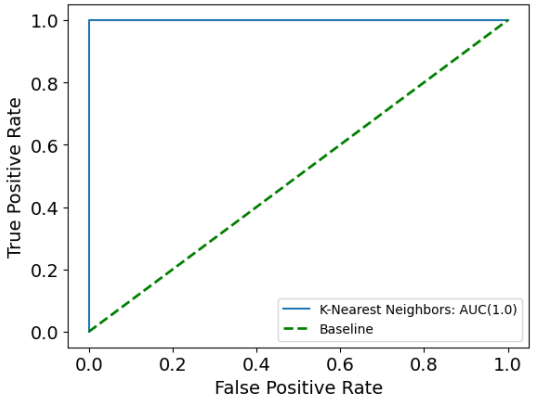

Fig. 4 A representation of the AUC curve to evaluate the binary classification of the KNN model.

TABLE I. Quantitative indicators to evaluate the prediction performance of the KNN and comparison to other machine learning models on binary classification.

Indicators	This work (%)	Other works (%)		
		KNN [6]	SVM [11]	SVM+DT+ANN [13]
Accuracy	100	95.00	90.3	99.5
Sensitivity	100	93.8	92.9	94.8
Precision	100	90.5	-	100.0
Specificity	100	-	88.2	94.83
F1-Score	100	92.1	89.7	95.2

TABLE II. Comparison of training and testing scores to evaluate overfitting and underfitting of the KNN model.

Train Score	100%
Test Score	100%

IV. Conclusions

This study successfully demonstrates the integration of machine learning into surface plasmon resonance imaging (SPRi) as a viable strategy to enhance the diagnostic performance of label-free biosensors. By leveraging a K-nearest neighbors (KNN) classifier trained on an augmented dataset of SPRi images, we achieved perfect classification accuracy, sensitivity, and precision, all within a computation time of under five seconds. This high performance was attributed to both the effective preprocessing of image data and the linear separability of the underlying features, reinforcing the role of data-driven models in biosensing.

The machine learning-enhanced SPRi platform showed exceptional potential for real-time, automated detection of binding events, offering a robust alternative to conventional manual interpretation, which is often subject to human error and limited sensitivity. Importantly, the model's receiver operating characteristic (ROC) curve exhibited an area under the curve (AUC) of 1.0, classifying it within the highest performance tier. These results not only validate the feasibility of using simple ML models in optical biosensing but also suggest that more complex models (e.g., convolutional neural networks) may yield further improvements when scaled to larger, more diverse datasets.

By automating the classification process and enhancing signal clarity, this work contributes to the evolution of intelligent, next-generation SPR-based biosensors. Such systems have the potential to revolutionize point-of-care diagnostics by enabling rapid, accurate, and reproducible biomolecular detection in clinical and environmental settings. Future studies should explore the generalizability of the model across different SPRi setups and incorporate transfer learning or deep learning approaches to handle larger datasets and more complex classification tasks.

Acknowledgement

We acknowledge the Department of Science, Technology and Innovation (DSTI) and the Council for Scientific and Industrial Research (CSIR) for funding this research. K. Mpofu was also supported by the South African Quantum Technology Initiative (SAQuTi) and the South African Medical Research Council (SAMRC).

References

[1] C.L. Wong, and M. Olivo, "Surface Plasmon Resonance Imaging Sensors: A Review". Plasmonics, vol. 9, pp. 809-824, February 2021.

[2] R . D'Agata, N. Bellassai, and G. Spoto. "Exploiting the design of surface plasmon resonance interfaces for better diagnostics: A perspective review". Talanta, Jan. 2024. [Online]. Available from: http://dx.doi.org/10.1016/j.talanta.2023.125033

[3] S. Kaziz, F. Echouchene, M.H. Gazzah. "Optimizing PCF-SPR sensor design through Taguchi approach, machine learning, and genetic algorithms". Scientific Reports, Apr. 2024. [Online] Available from: http://dx.doi.org/10.1038/s41598-024-55817-9

[4] Y. Fang. "Label-Free Biosensors for Cell Biology". Int. J. Electrochem. Sci. vol. 11, pp. 1–16. 2011

[5] G.A. González, G. Rattá, D. Gadariya, and S. Domrido. "Advancing Marfe Detection in Jet's Operational Camera Videos Through Machine Learning Techniques". 2023. [Online] Available from: http://dx.doi.org/10.2139/ssrn.4639605

[6] K. Moon, and A. Jetawat. "Predicting Lung Cancer with K-Nearest Neighbors (KNN): A Computational Approach", Ind. J. Sci. Technol. Vol. 25, pp, 2199–2206, May 2024.

[7] A.A. Amer, S.D. Ravana, and R.A.A. Habeeb. "Effective k-nearest neighbor models for data classification enhancement", Int. Indian J. Big Data, vol. 12, p. 86, Apr. 2025.

[8] R.K. Sachdeva, P. Bathla, P. Rani, R. Lamba, G.S.P. Ghantasala, and I.F. Nassar. "A novel K-nearest neighbor classifier for lung cancer disease diagnosis", Neural Comput. Appl., vol. 36, pp. 22403–22416, Sep. 2024.

[9] S.I. Nafisah, and G. Muhammad. "Tuberculosis detection in chest radiograph using convolutional neural network architecture and explainable artificial intelligence". Neural Comput. Appl., vol. 36, pp. 111–131, Apr. 2022.

[10] L . An, K. Peng, X. Yang, P. Huang, Y. Luo, and P. Feng, "E-TBNet: Light Deep Neural Network for Automatic Detection of Tuberculosis with X-ray DR Imaging", Sensors, vol. 22, p. 821, Jan. 2022.

[11] N. Tsebesebe, K. Mpofu, S. Ndlovu, S. Sivarasu, and P. Mthunzi-Kufa, "Detection of SARS-CoV-2 from raman spectroscopy data using machine learning models", In MATEC Web of Conferences, vol. 388, p. 07002, Oct. 2023.

[12] N. Tsebesebe, K. Mpofu, S. Ndlovu, S. Sivarasu, and P. Mthunzi-Kufa,. (2024). "Predicting gene families from human DNA sequences using machine learning: a logistic regression approach". Comput. Opt. Imaging Artif. Intell. Biomed. Sci., vol. 12857, pp. 100-106, Jan. 2024.

[13] N. Tsebesebe, K. Mpofu, S. Ndlovu, S. Sivarasu, and P. Mthunzi-Kufa, "Majority voting algorithm for TB detection: Machine learning approach", in The Proceedings of SAIP2023, pp. 297– 304, Jul. 2023.

[14] HORIBA, "Scientific and Analytical Instruments", 2025. [Online] Available: https://www.horiba.com/int/scientific/technologies/surface-plasmon-resonance-imaging/surface-plasmon-resonance-imaging/